



## Detection of an ultralow velocity zone at the core-mantle boundary using diffracted $PKKP_{ab}$ waves

Sebastian Rost<sup>1</sup> and Edward J. Garnero<sup>1</sup>

Received 27 May 2005; revised 16 January 2006; accepted 8 March 2006; published 27 July 2006.

[1] Seismic phases diffracted around Earth's core contain information about lowermost mantle wave speeds. By measuring the slowness of incident diffracted energy from array recordings, seismic velocity along the diffracted path can be estimated. Here we apply this principle to diffraction of the major arc seismic phase  $PKKP_{ab}$  recorded at the Canadian Yellowknife array to estimate  $P$  wave velocity variations along the core-mantle boundary. We observe  $PKKP_{ab}^{diff}$  about  $7.5^\circ$  past the ray theoretical cutoff distance for  $PKKP_{ab}$ . We utilize 330 western Pacific rim earthquakes that allow us to probe the core-mantle boundary beneath the North Atlantic and the South Pacific oceans using  $PKKP_{ab}^{diff}$ . Slowness and back azimuth are measured by frequency–wave number analysis. Mapping  $PKKP_{ab}^{diff}$  slowness variations suggest 4–19%  $P$  wave velocity reductions relative to PREM, in good agreement with the magnitude of velocity reductions previously mapped in ultralow velocity zones. The  $PKKP_{ab}^{diff}$  slowness and back-azimuth variations combined with results from previous ULVZ studies using  $SP_{diff}KS$  imply that the lowered velocities occur at the base of the mantle beneath the North Atlantic Ocean, along the receiver side of raypaths.  $PKKP_{ab}^{diff}$  array measurements thus hold important potential for mapping ultralow velocity zone structure in so far unprobed regions of the lower mantle as well as for providing additional and independent information about lower mantle structure.

**Citation:** Rost, S., and E. J. Garnero (2006), Detection of an ultralow velocity zone at the core-mantle boundary using diffracted  $PKKP_{ab}$  waves, *J. Geophys. Res.*, *111*, B07309, doi:10.1029/2005JB003850.

### 1. Introduction

[2] Strong elastic heterogeneities have been mapped close to the core-mantle boundary (CMB) over the last 20 years (see Garnero [2000] for a recent review). Detected structures include a discontinuity on top of the  $D''$  layer [Lay and Helmberger, 1983; Young and Lay, 1990; Wysession et al., 1998] perhaps due to a phase transition in perovskite [Murakami et al., 2004; Lay et al., 2005], anisotropy in  $D''$  [Kendall and Silver, 1996; Lay et al., 1998; Kendall, 2000], strong reductions of seismic velocities in ultralow velocity zones (ULVZ) [Garnero and Helmberger, 1996; Revenaugh and Meyer, 1997; Thorne and Garnero, 2004; Rost et al., 2005], strong scattering of seismic energy [Vidale and Hedlin, 1998; Wen and Helmberger, 1998; Hedlin and Shearer, 2000] and rigid layers at the top of the outer core [Buffett et al., 2000; Rost and Revenaugh, 2001]. The large variety of heterogeneities found at or near the CMB is not unexpected for such a major thermal and chemical boundary layer in the Earth's interior. Despite the large number of seismic studies of CMB structure, many questions of the evolution and dynamics of structural

features at the CMB remain open. Additionally, large areas of the CMB have not yet been probed.

[3] ULVZ are one of the most enigmatic features found at the CMB. Lateral scale lengths of ULVZ range from several thousands of kilometers [Garnero et al., 1998; Thorne and Garnero, 2004] to tens of kilometers [Rost and Revenaugh, 2003a; Rost et al., 2005]. ULVZ thickness have been mapped between 4 to 50 km with  $P$  wave and  $S$  wave reductions of 5 to 40% [Revenaugh and Meyer, 1997; Garnero, 2000; Rost and Revenaugh, 2003a; Thorne and Garnero, 2004], and a notable increase of density has also been inferred [Rost et al., 2005; Garnero et al., 2006].

[4] Several interesting features of ULVZ include their nonglobal occurrence, clear ULVZ detections often in close proximity to ULVZ nondetections [Persh et al., 2001; Thorne and Garnero, 2004; Rost and Revenaugh, 2003a; Rost et al., 2005], and their difference in  $P$  and  $S$  wave velocity reductions [Castle and van der Hilst, 2000]. Because of restrictions of source-receiver combinations and a limited number of seismic phases sensitive to ULVZ structure, many regions of the Earth have not been probed for ULVZ structure so far. Nonetheless, to better understand the dynamics and evolution of ULVZ and their role in mantle convection, a more complete sampling of the CMB for possible ULVZ regions and their seismic properties is essential.

[5] Here we propose to use the diffracted path of  $PKKP_{ab}$ , a phase observed up to several degrees beyond

<sup>1</sup>Department of Geological Sciences, Arizona State University, Tempe, Arizona, USA.

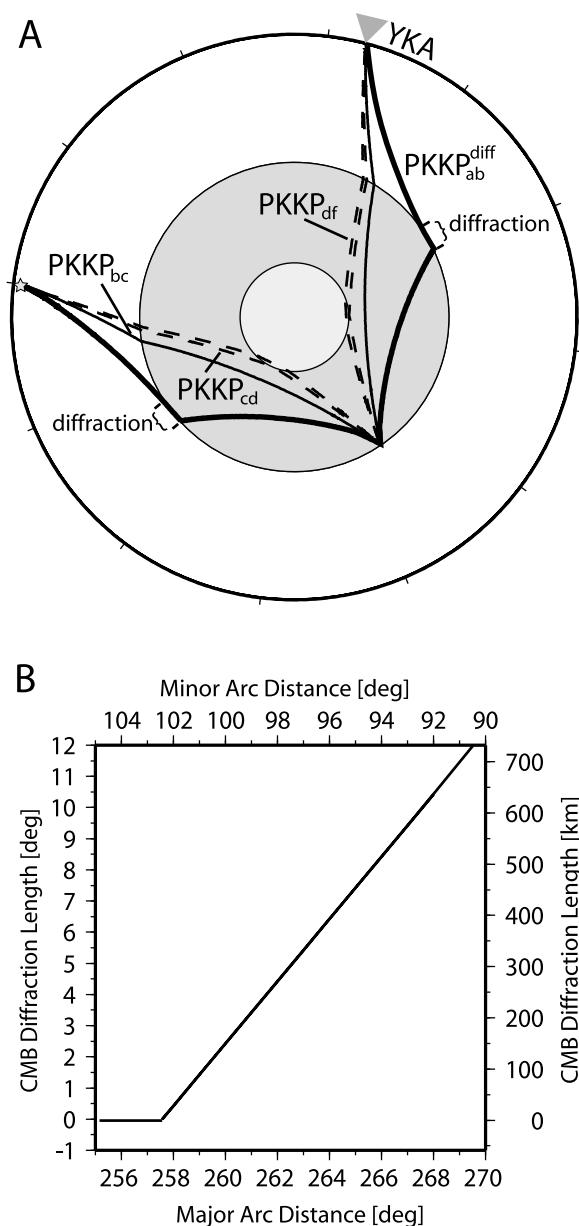


**Figure 1.** (a) Raypaths for  $PKKP$ ,  $PKKP_{bc}$  and  $PKKP_{ab}^{diff}$  raypaths are shown as solid lines, and raypaths for  $PKKP_{cd}$  and  $PKKP_{df}$  are shown as dashed lines. Raypaths are calculated for an event (star) with minor arc distance of  $98^\circ$  (major arc distance  $262^\circ$ ) to the Yellowknife array (inverted triangle); event depth is 50 km. For this epicentral distance,  $PKKP_{ab}^{diff}$  includes  $4.4^\circ$  of diffraction along the CMB. The paths of  $PKKP_{bc}$  and  $PKKP_{ab}^{diff}$  in the mantle are quite different, so that  $PKKP_{bc}$  cannot be used as a reference phase. (b) Total diffraction path length in degrees and kilometers of  $PKKP_{ab}^{diff}$  versus minor and major arc epicentral distances for a surface focus earthquake in the PREM model.

its ray theoretical distance of termination, to map the seismic velocities at the CMB. In particular, the slowness of short-period  $PKKP_{ab}^{diff}$  arrivals, provide a constraint on the small-scale seismic velocity variations at the CMB.

$PKKP_{ab}^{diff}$  samples lower mantle regions that are not accessible by phases like  $PcP$  or  $ScP$  with current earthquake-receiver geometries; also,  $PKKP_{ab}^{diff}$  can be used in combination with phases like  $SP_{diff}KS$  to improve constraints on ULVZ structure. Diffracted  $P$  wave phases have been used to map structures in the lowermost mantle before [e.g., Okal and Geller, 1979; Mula and Müller, 1980; Wysession and Okal, 1989; Young and Lay, 1990; Bataille and Lund, 1996; Wysession, 1996; Wysession et al., 1999], though these efforts primarily focused on bulk  $D''$  properties.

[6] In the next section, we introduce ULVZ modeling with  $PKKP_{ab}^{diff}$ , as well as constraints and uncertainties of this phase. This is followed by an investigation of CMB structure in the North Atlantic using array analysis of

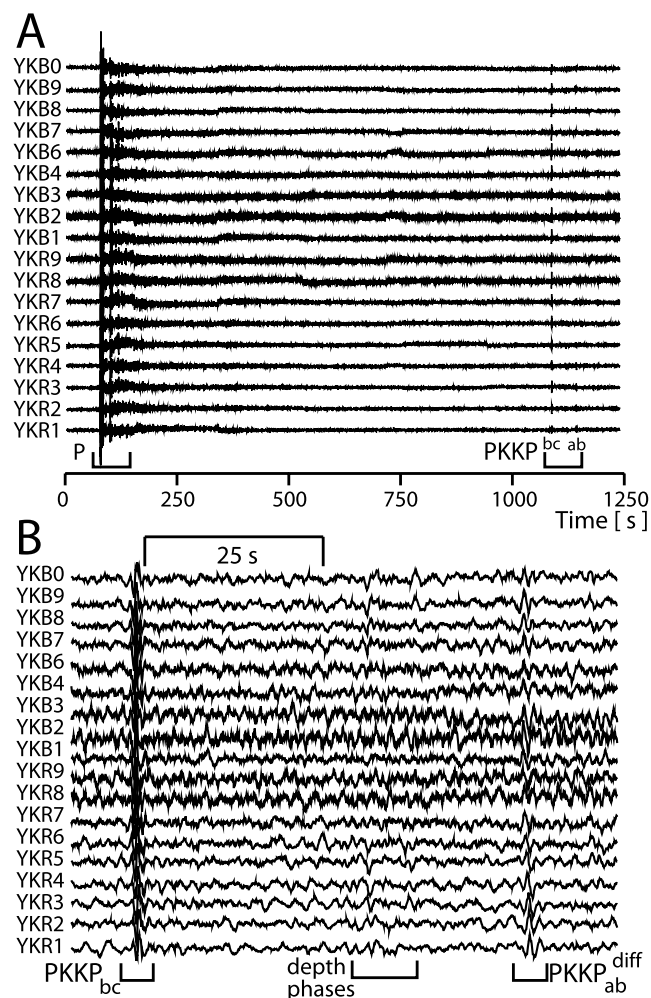


**Figure 2.** (a) Raw YKA recordings for the event on 1 April 1991, 0525 UT (source depth  $h = 90$  km). The time window from  $P$  to  $PKKP$  for all 18 recording stations of the array are shown. Epicentral distance to YKA is  $95.63^\circ$ , with a back azimuth of  $270.35^\circ$ . Recordings of the short-period vertical instruments with a dominant period of  $\sim 1$  s are shown. (b) Zoom into the  $PKKP$  time window for the same event. Amplitudes are normalized to the  $PKKP_{bc}$  amplitudes. Note the apparent lower-frequency content of  $PKKP_{ab}^{diff}$  due to the loss of higher frequencies from diffraction.

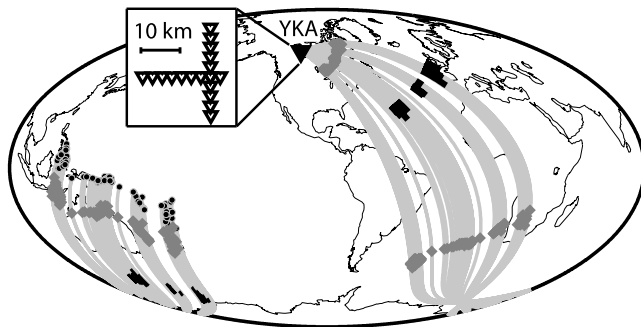


**Figure 3.** Earthquake (circles) to receiver (YKA, triangle) geometries for data analyzed in this study. Also shown are  $PKKP$  raypaths along the major arc of the great circle path (gray lines) and  $PKKP_{bc}$  CMB entry, exit, and midreflection points (gray diamonds). Diffracted arc lengths  $PKKP_{ab}^{diff}$  for earthquakes in Table 1 are also shown (thick black line segments). Shown are the full diffracted path lengths on both the sources and receiver side of  $PKKP_{ab}^{diff}$ .

$PKKP_{ab}^{diff}$  where we document slowness and traveltime anomalies to infer strong and variable ULVZ properties.

## 2. $PKKP_{ab}^{diff}$

[7]  $PKKP$  is a  $P$  wave that travels along the major arc of the great circle path (Figure 1a). It consists of two mantle  $P$  wave legs and two core  $P$  wave legs with a reflection at the underside of the CMB. The ray theoretical cutoff epicentral distance for  $PKKP_{ab}$  for a surface focus earthquake in the PREM reference model [Dziewonski and Anderson, 1981] is approximately  $102.42^\circ$  (minor arc distance). Diffraction of  $PKKP_{ab}$  occurs for shorter minor arc epicentral distances, since  $PKKP_{ab}$  travels along the major arc of the path (Figure 1b). In the remainder of this paper we always refer to minor arc distances. In theory, the diffraction can occur at either the source or receiver sides (or both) of the raypath (Figure 1a shows equal length diffraction segments).

[8]  $PKKP$  has been used to study CMB structure in past studies [Doornbos, 1980; Earle and Shearer, 1997; Rost and Revenaugh, 2003b].  $PKKP$  energy is dominant in short-period seismograms and is often the dominant phase arriving about 1000s after direct  $P$  (see Figure 2). The traveltime branches of the  $PKKP$  triplication ( $PKKP_{ab}$ ,  $PKKP_{bc}$ ,  $PKKP_{cd}$  and  $PKKP_{df}$ ) can often be easily identified, although  $PKKP_{df}$  and  $PKKP_{cd}$  are sometimes difficult to detect due to their low amplitude. The  $PKKP_{ab}$  and  $PKKP_{bc}$  branches are separated by a slowness difference of approximately 1.5 s/deg (which slightly varies with epicentral distance). These slowness differences can easily be resolved in short-period data from small or medium aperture arrays with apertures of a few tens of kilometers.

## 3. Short-Period Array Data Set

[9] We collected data from more than 330 western Pacific rim earthquakes deeper than 60 km recorded at the Yellowknife array (YKA). This Canadian array has an aperture of 20 km and consists of 18 short-period vertical component instruments (Figure 3). This selection represents all seis-

micity with a magnitude larger than 5.5 in the appropriate distance range for  $PKKP_{ab}^{diff}$  ( $89^\circ$ – $117^\circ$ ) from the western Pacific from September 1989 to March 1996. Data were checked for obvious errors such as spikes and instrument outage and then band-pass filtered with a narrow filter between 0.5 Hz and 1.4 Hz optimizing the signal-to-noise ratio of  $PKKP$ .

[10] We use phase-weighted stacking (PWS) [Schimmel and Paulssen, 1997] for better identification of  $PKKP$  arrivals in slowness-time space and precise traveltime measurements. We were able to detect  $PKKP_{ab}^{diff}$  and/or  $PKKP_{bc}$  arrivals in recordings of 131 earthquakes. We exclude earthquakes with distances larger than  $104^\circ$  where

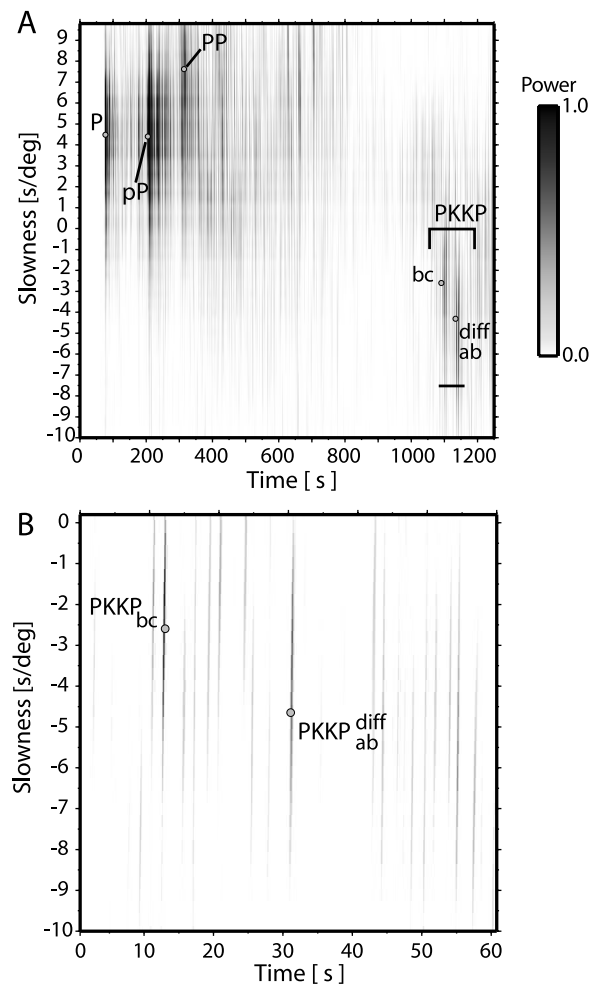


**Figure 4.** (a) Third-power phase-weighted stack for the earthquake on 9 March 1994, 2328 UT with epicentral distance of  $94.3^\circ$ . Traveltimes for the PREM model and major phases ( $P$ ,  $pP$ ,  $PP$ , and  $PKKP$ ) are marked.  $PKKP_{bc}$  and  $PKKP_{ab}^{diff}$  are dominant phases in the short-period recordings and can be easily identified in the time-slowness plots. The inset shows the  $PKKP$  time and slowness window. The two major arrivals of  $PKKP_{bc}$  and  $PKKP_{ab}^{diff}$  with slownesses of approximately 2.6 and 4.4 s/deg, respectively, can be identified. (b) Zoom into the  $PKKP$  time and slowness window. Arrivals for  $PKKP_{bc}$  and  $PKKP_{ab}^{diff}$  are marked. The zoom window location is marked by a horizontal line in Figure 4a.

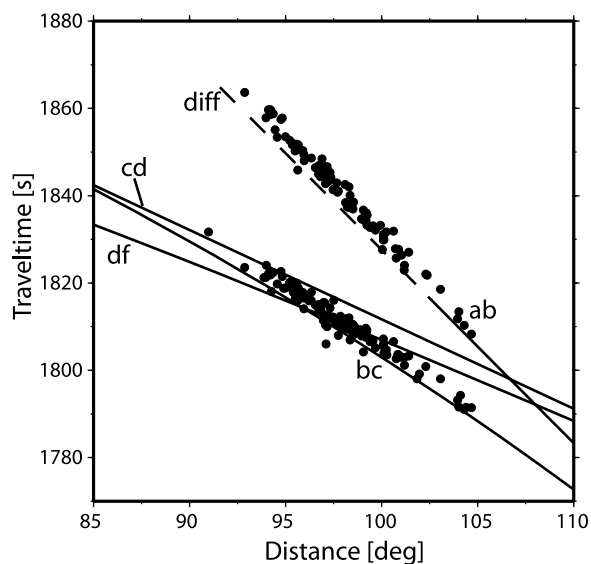


**Figure 5.** Traveltime measurements for the data set in Figure 3 for  $PKKP_{bc}$ ,  $PKKP_{ab}$ , and  $PKKP_{ab}^{diff}$ . Lines denote theoretical PREM predictions for the individual  $PKKP$  traveltime branches. The dashed line denotes the theoretical traveltime of  $PKKP_{ab}^{diff}$ . Traveltime deviations in excess of 3 s relative to PREM are observed with slightly larger delays observed for  $PKKP_{ab}^{diff}$ . The  $bc$  traveltimes show stronger scatter in the traveltimes than  $PKKP_{ab}^{diff}$  ( $PKKP_{ab}$ ).

no  $PKKP_{ab}^{diff}$  arrivals are expected (e.g., Figure 1b). The raypaths for these 131 events are shown in Figure 3. The CMB diffracted path lengths are shorter than about  $7.5^\circ$  or less than 455 km at the CMB.

[11] Third-power PWS [Schimmel and Paulssen, 1997] processed data are shown in Figure 4 and show that slowness differences between  $PKKP_{bc}$  and  $PKKP_{ab}^{diff}$  are easily resolvable.  $PKKP$  traveltimes are measured in the PWS stacked data (Figure 5). Traveltime measurements are accurate to 0.2 s.

[12] To estimate seismic velocities along the CMB, events with a signal-to-noise ratio of  $PKKP_{ab}^{diff}$  larger than 3 were selected. In total, 26 events meet this criterion (see Table 1 for a listing of event details). For these events,  $PKKP_{ab}^{diff}$  can be identified in single seismograms (as in Figure 2). Using frequency–wave number analysis [Capon, 1973], the slowness and back azimuth were measured for these events (Figures 6 and 7). These measurements will be used in the following to determine the  $P$  wave velocity along the diffracted path.

#### 4. Analysis and Results

[13] We measure traveltimes of dominant arrivals ( $P$ ,  $P_{diff}$ ,  $PKiKP$ ,  $PKKP_{bc}$  and  $PKKP_{ab}^{diff}$ ) in the 131 earthquakes that show  $PKKP$  energy in the 3rd power PWS. The event information for these events is given in the auxiliary material<sup>1</sup>. Figure 5 shows traveltimes for  $PKKP_{ab}$  and  $PKKP_{bc}$  (the measurements for  $P$  and  $PKiKP$  are omitted

for clarity). The traveltimes were corrected for source depth differences using the PREM model.  $PKKP_{bc}$  and  $PKKP_{ab}^{diff}$  traveltimes display significant variability (Figure 5).  $PKKP_{bc}$  arrives on average about 3 s and  $PKKP_{ab}$  about 4 s later than predicted by PREM, indicating three-dimensional wave speed variations along the  $PKKP$  paths. The traveltimes of  $PKKP_{ab}^{diff}$  are a clear continuation of the  $PKKP_{ab}$  traveltime branch beyond the ray theoretical termination at about  $102^\circ$  defining the start of the diffracted path.

[14] Results of the fk analysis for  $PKKP_{bc}$  and  $PKKP_{ab}^{diff}$  are shown in Figure 6.  $PKKP_{ab}^{diff}$  shows in general larger slownesses than predicted by PREM with an average of  $+0.53 \pm 0.22$  s/deg. Back azimuth varies with variations of  $0.2^\circ \pm 3.9^\circ$ . Despite the small overall back-azimuth variation, there are some trends observable in the back-azimuth deviations for  $PKKP_{ab}^{diff}$ . However, these deviations are below the back-azimuth resolution of the medium-aperture YKA, which has been found to be able to resolve back-azimuth variations of approximately  $\pm 8^\circ$  [Rost and Weber, 2001]. We find that slowness variations for  $PKKP_{ab}^{diff}$  are in the range of 0.2 to 0.8 s/deg. Slowness variations of this scale can be easily detected and resolved by YKA [Rost and Weber, 2001].

[15] Slowness and back-azimuth measurements for  $PKKP_{bc}$  from the same recordings show stronger and more complicated variations, especially for back azimuths smaller than  $260^\circ$ . Back-azimuth deviations are dominantly toward the east. In contrast to  $PKKP_{ab}^{diff}$  the  $PKKP_{bc}$  back-azimuth deviations for back azimuths smaller than  $260^\circ$  can be easily resolved by YKA. Slowness perturbations of  $PKKP_{bc}$  are larger and smaller than those predicted by PREM, without any apparent geographical systematics, in contrast to  $PKKP_{ab}^{diff}$  where only larger slownesses than PREM are

**Table 1.** Earthquake Information for Large-Amplitude  $PKKP^a$

Origin	Latitude, deg	Longitude, deg	Depth, km
7 Dec 1989, 1338 UT	-6.450	146.412	117.69
18 Feb 1990, 1221 UT	-5.550	149.447	150.27
2 May 1990, 2250 UT	-5.666	150.199	92.29
29 Jun 1990, 0353 UT	-21.310	-179.410	618.00
22 Jul 1990, 0926 UT	-23.654	-179.849	543.73
18 Apr 1991, 0941 UT	-22.923	-179.263	476.07
3 Dec 1991, 1033 UT	-26.518	178.751	571.67
7 Apr 1992, 0337 UT	-4.192	130.960	51.00
11 Jul 1992, 1044 UT	-22.498	-178.294	388.91
16 Aug 1992, 1023 UT	-5.331	146.763	215.00
15 Sep 1992, 2104 UT	-14.083	167.279	193.48
12 Nov 1992, 2228 UT	-22.390	-178.008	365.57
16 Apr 1993, 1408 UT	-17.760	-178.797	564.18
7 Aug 1993, 1753 UT	-23.900	179.954	520.00
11 Feb 1994, 2117 UT	-18.773	169.259	213.07
31 Mar 1994, 2240 UT	-22.071	-179.433	588.85
17 Jan 1995, 1654 UT	-20.830	-179.240	634.00
12 Mar 1995, 1209 UT	-5.325	146.804	230.12
24 Jun 1995, 0658 UT	-3.960	153.930	386.00
3 Jul 1995, 2156 UT	-29.120	-177.630	54.00
14 Aug 1995, 0437 UT	-4.840	151.520	128.00
2 Mar 1996, 0150 UT	-5.970	146.570	59.00
17 Mar 1996, 1448 UT	-14.710	167.300	164.00
15 Apr 1996, 1455 UT	-6.190	154.830	56.00
16 Apr 1996, 0030 UT	-24.060	-177.040	111.00
10 Jun 1996, 0104 UT	-13.480	167.130	200.00

<sup>a</sup>Shown is earthquake location information for the selected high-amplitude  $PKKP_{ab}^{diff}$  events that were used to measure slowness and back azimuth of  $PKKP_{ab}^{diff}$ .

<sup>1</sup>Auxiliary material is available at <ftp://ftp.agu.org/apend/jb/2005jb003850>.

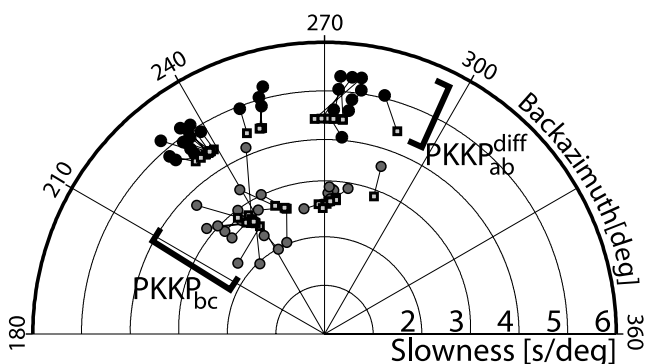


**Figure 6.** Slowness–back-azimuth measurements in polar coordinates for events with good  $PKKP_{ab}^{diff}$  SNR, as measured with fk analysis. Theoretical (PREM) values for  $PKKP_{bc}$  and  $PKKP_{ab}^{diff}$  are indicated by squares.  $PKKP_{bc}$  measurements are marked as gray circles, and  $PKKP_{ab}^{diff}$  are marked as black circles.  $PKKP_{bc}$  shows overall stronger variability in the measurements.  $PKKP_{ab}^{diff}$  shows larger-than-PREM slowness, indicating lower  $P$  wave velocities along the diffracted path at the CMB.

observed.  $PKKP_{bc}$  traveltimes in the distance range from  $95^\circ$  to  $105^\circ$  are very similar to phases traversing ( $PKIKKIKP$  or  $PKKP_{df}$ ) and reflecting off the inner core ( $PKiKKiKP$  or  $PKKP_{cd}$ ) (Figure 1) with slownesses of about 1.8 s/deg and 2.0 s/deg, respectively. Interference of  $PKKP_{bc}$  with these phases could also influence its slowness, depending on the amplitudes of  $PKKP_{df}$  and  $PKKP_{cd}$ .

[16] Measuring  $PKKP_{ab}^{diff}$  slowness and back azimuth relative to  $PKKP_{bc}$  allows estimating the influence of structure close to source and receiver. We observe that relative slowness variations of  $PKKP_{ab}^{diff}$  are comparable to the ones shown in Figure 6, indicating that structure close to source and receiver (which are sampled by  $PKKP_{ab}^{diff}$  and  $PKKP_{bc}$ ) are not the main source for the slowness variations.

[17] Slowness and back-azimuth measurements from seismic arrays are strongly influenced by lateral variations of the seismic structure beneath the arrays [Krüger and Weber, 1992]. YKA shows very small mislocation vectors [Bondar et al., 1999] and the structure beneath the array has been found to be simple with an almost constant Moho depth of 39.4 km [Bank et al., 2000]. We can also rule out intra-array topography as source for the slowness variations, since YKA shows only station elevations from 170 m (station YKR1) to 221.6 m (station YKB0). We conclude that near source and receiver structure are unlikely to bias the slowness measurements and the slowness variations indeed originate from structures in the deep mantle.

[18] Since the mantle paths (and core entry and exit points) of  $PKKP_{bc}$  and  $PKKP_{ab}^{diff}$  differ strongly (Figure 1) a direct comparison of  $PKKP_{ab}^{diff}$  and  $PKKP_{bc}$  to resolve CMB or lower mantle structure is not possible. Strong variations in mantle velocities along the  $PKKP_{bc}$  path are necessary to explain the significant slowness and back-azimuth scatter seen in Figure 6. It is likely that  $PKKP_{ab}^{diff}$  shows less slowness and back-azimuth variation since the receiver side path is restricted to be along the CMB due to

diffraction. Thus the upgoing  $PKKP_{ab}^{diff}$  energy should represent the slowness for diffracted energy along the CMB.

[19] Apparent velocities  $v_0$  at the CMB from the measured  $PKKP_{ab}^{diff}$  slownesses  $u$  can be calculated using  $u = \frac{R_0 \cdot \sin(i)}{v_0}$  with  $R_0 = \frac{R_E - r}{R_E}$  and  $r$  being the depth of the diffracted ray path,  $R_E$  being the radius of the Earth. Figure 7a shows the distribution of inferred velocity changes (relative to PREM) along the diffracted paths. The velocity changes are only shown at the receiver side of the path, while the source side paths are marked by red lines (Figure 7b shows a magnification of the sampled receiver side patch). Because of the reciprocity of the seismic path, both the source and receiver CMB entry points and the CMB underside reflection points can be the region where diffraction happens. We checked waveforms

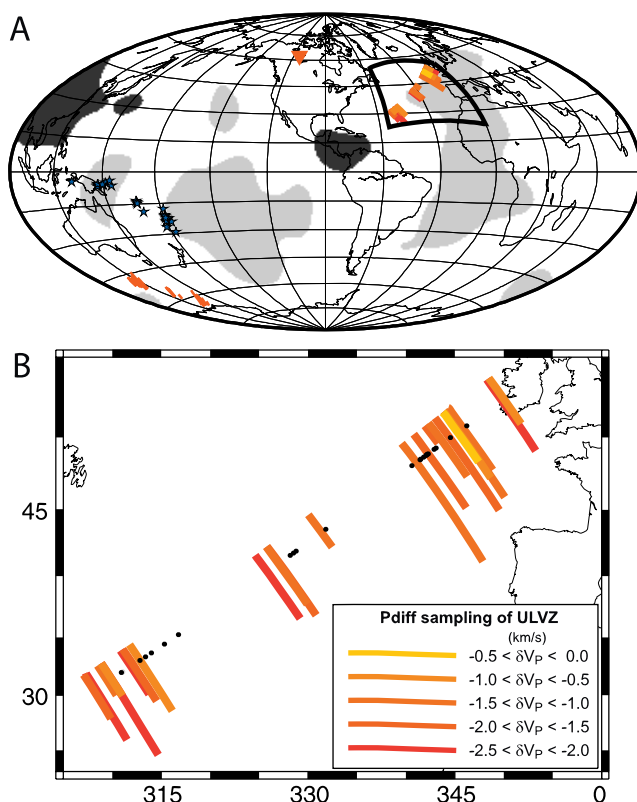


**Figure 7.** (a)  $P$  wave velocity reductions along diffracted portions of  $PKKP_{ab}^{diff}$  paths. Sources (stars) and the YKA receiver array (triangle) are marked.  $P$  wave velocity reductions are shown along the receiver side diffracted path. For simplicity, the source-side diffracted paths are shown as lines without showing the velocity reductions. The background  $P$  wave velocity variations are for the  $D''$  layer from Kárason and van der Hilst [2001]. Only regions with  $|\delta V_P| > 0.4$  are shown, with velocity reductions shown as light gray and increases shown in dark gray. (b) Magnification (region shown as box in Figure 7a) of the receiver side  $PKKP_{ab}^{diff}$  paths with lines denoting the velocity reductions along the diffracted portions of  $PKKP_{ab}^{diff}$ . Black circles show the ray theoretical termination point of  $PKKP_{ab}^{diff}$  for the theoretical back azimuth and PREM diffracted slowness. Western  $P_{diff}$  shows stronger departures from the ray theoretical exit points than those farther to the east.

for dual  $PKKP_{ab}^{diff}$  onsets, which would indicate different speeds of diffraction on the source and receiver sides of the  $PKKP_{ab}$  path. For example a combination of a PREM and non-PREM (e.g., ULVZ) CMB velocity structure at the source and receiver side of the  $PKKP_{ab}^{diff}$  path would produce multiple onsets. The absence of such waveform anomalies may indicate a focusing of the energy along the CMB in a ULVZ waveguide on one side of the path yielding high (and observable) amplitudes of  $PKKP_{ab}^{diff}$  or similar velocity structures along both diffracted legs. All  $PKKP_{ab}^{diff}$  waveforms in our data set show single arrivals with waveforms similar to  $P$ , and similar to a Hilbert-transformed  $PKKP_{bc}$ , as expected [Doornbos, 1980]. An earlier study of CMB ULVZ structure [Thorne and Garnero, 2004] indicates that the region beneath the southern Pacific Ocean does not show evidence for strong ULVZ structure, while the studied area beneath the northern Atlantic Ocean likely contains ULVZ at the CMB [Thorne and Garnero, 2004]. Additionally,  $PKKP_{ab}^{diff}$  shows much smaller back-azimuth deviations from theoretical predictions than  $PKKP_{bc}$ . The strongest heterogeneities in the Earth are found in the upper mantle (where the raypaths of  $PKKP_{bc}$  and  $PKKP_{ab}^{diff}$  are very similar) and at the CMB (where the two paths differ the most) [e.g., Lay et al., 2004]. The small back-azimuth variations of  $PKKP_{ab}^{diff}$  suggest the diffracted leg is not located at the source side of the path, as this would result in larger variations toward the end of the  $PKKP_{ab}^{diff}$  path. We therefore assume that the anomalous diffraction observed here is limited to the receiver side of  $PKKP_{ab}^{diff}$  paths. Further studies using  $PKKP$  and other CMB probes that result in crossing paths will give more constraints on the location of the anomalous velocity structure.

[20] The small grey circles in Figure 7b mark the ray theoretical end-points of the diffracted paths for PREM slowness and back-azimuth values. The back-azimuth deviations are in agreement with the ones shown in Figure 6, with stronger deviations to the west. The shortest diffracted segments in this region show the smallest decrease of apparent velocity, which is consistent with an integrative effect along the diffracted path segment. The eastern and center portions of the study area show slightly smaller reductions (0–10%), again the shorter paths in this regions show smaller velocity reductions.

## 5. Discussion and Conclusions

[21] The calculated  $P$  velocity reductions at the CMB are between 4 to 19 ( $\pm 4$ )% relative to PREM. These reductions are significantly larger than those inferred for  $D''$  from longer period diffracted phases, which are in the range of 2% [e.g., Wysession et al., 1999], and more similar to reductions reported for ULVZ reductions [Mori and Helmberger, 1995; Garnero and Helmberger, 1996; Rost and Revenaugh, 2003a]. The shorter periods used in this study are sensitive to finer-scale ULVZ structure due to their smaller Fresnel volume. Unfortunately, we lack independent information about the thickness of the ULVZ in this region. A minimum thickness of about 10 to 20 km can be inferred from the  $\sim 13$  km wavelength of the data with 1 s dominant period. The velocity reductions mapped in Figure 7 show some complicated, fine-scale structure that makes it difficult to find one model to fit the observations. Both the location

and the length of the diffracted paths affect the apparent velocity reductions. Nonetheless, this type of variation within general ULVZ locales is similar to that seen in previous studies [e.g., Garnero and Helmberger, 1996; Thorne and Garnero, 2004]. Figure 7a also shows  $P$  wave tomography [Kárason and van der Hilst, 1999] with velocity variations  $|\delta V_P| > 0.4\%$  in grey shading, indicating that we sample the edge of a very slow region of the Earth. The slow region may be the northern extension of the South African anomaly [Ni and Helmberger, 2003; Wang and Wen, 2004]. It has been speculated that these structures are thermochemical piles [Wen et al., 2001; Wen, 2001; Tackley, 2002; McNamara and Zhong, 2004, 2005] and ULVZ have been detected at the boundaries of slow regions of the Earth's lower mantle before [Thorne et al., 2004; Rost et al., 2005]. There are indications that ULVZ primarily develop in the hot regions at the outer edges of these features [Garnero et al., 2006].

[22] Tomographic corrections for  $PKKP$  are much smaller than the measured traveltimes variations and traveltimes delays calculated from the detected ULVZ velocity reductions and are probably not the source for the slowness variations found in this study. For example, we find average traveltimes corrections due to mantle  $P$  wave structure for all source-receiver combinations with a mean of  $-0.18 (\pm 0.08)$  s for the model by Kárason and van der Hilst [2001]. Eastern events (with the westernmost receiver side CMB diffraction paths) show the largest corrections, between  $-0.2$  and  $-0.3$  s. Events further to the west (with diffracted paths further east) show small corrections between  $-0.1$  and  $-0.2$  s. This greatly underpredicts our  $PKKP_{ab}^{diff}$  delays, which change between 2 and 4 s.

[23] The area sampled by  $PKKP_{ab}^{diff}$  located in the northern Atlantic Ocean has been studied previously using  $SP_{diff}KS$  [Garnero et al., 1993; Helmberger et al., 1998, 2000; Thorne and Garnero, 2004] and has been found to show evidence for ULVZ. Indeed, data sampling the CMB slightly south of our study area show some very anomalous  $SP_{diff}KS$  waveforms due to a large amplitude postcursor that is best modeled by a strong ULVZ (M. Thorne, personal communication, 2005). Strong variability in ULVZ structure has been reported, which makes it difficult to distinguish between a continuous ULVZ layer (in larger-scale ULVZ areas) or ULVZ patches, as found in the work of Rost et al. [2005].

[24] We find that the ULVZ velocities are able to explain the traveltimes anomalies found for  $PKKP_{ab}^{diff}$  (Figure 3) as well as the slowness variations. A diffraction path length of  $4^\circ$  ( $7^\circ$ ) degrees through a ULVZ with 5 to 15%  $P$  wave velocity reductions will lead to traveltimes anomalies of 1 (1.6) seconds for a 5% velocity reduction and 3.1 (5.5) seconds for a 15%  $V_P$  anomaly, which are of the same order as observed in our data. Therefore our interpretation of the slowness deviations originating from ULVZ is consistent with the measured traveltimes delays.

[25] Although  $PKKP_{ab}^{diff}$  possesses the source-receiver ambiguity of distinguishing between the source or receiver diffracted paths as the source of anomalous observations, not unlike  $SP_{diff}KS$  or  $PKP$ , it holds potential to fill geographic gaps in the maps of ULVZ study areas due to its unique source-receiver geometry possibilities. The combination of  $PKKP_{ab}^{diff}$  with other ULVZ probes, such as

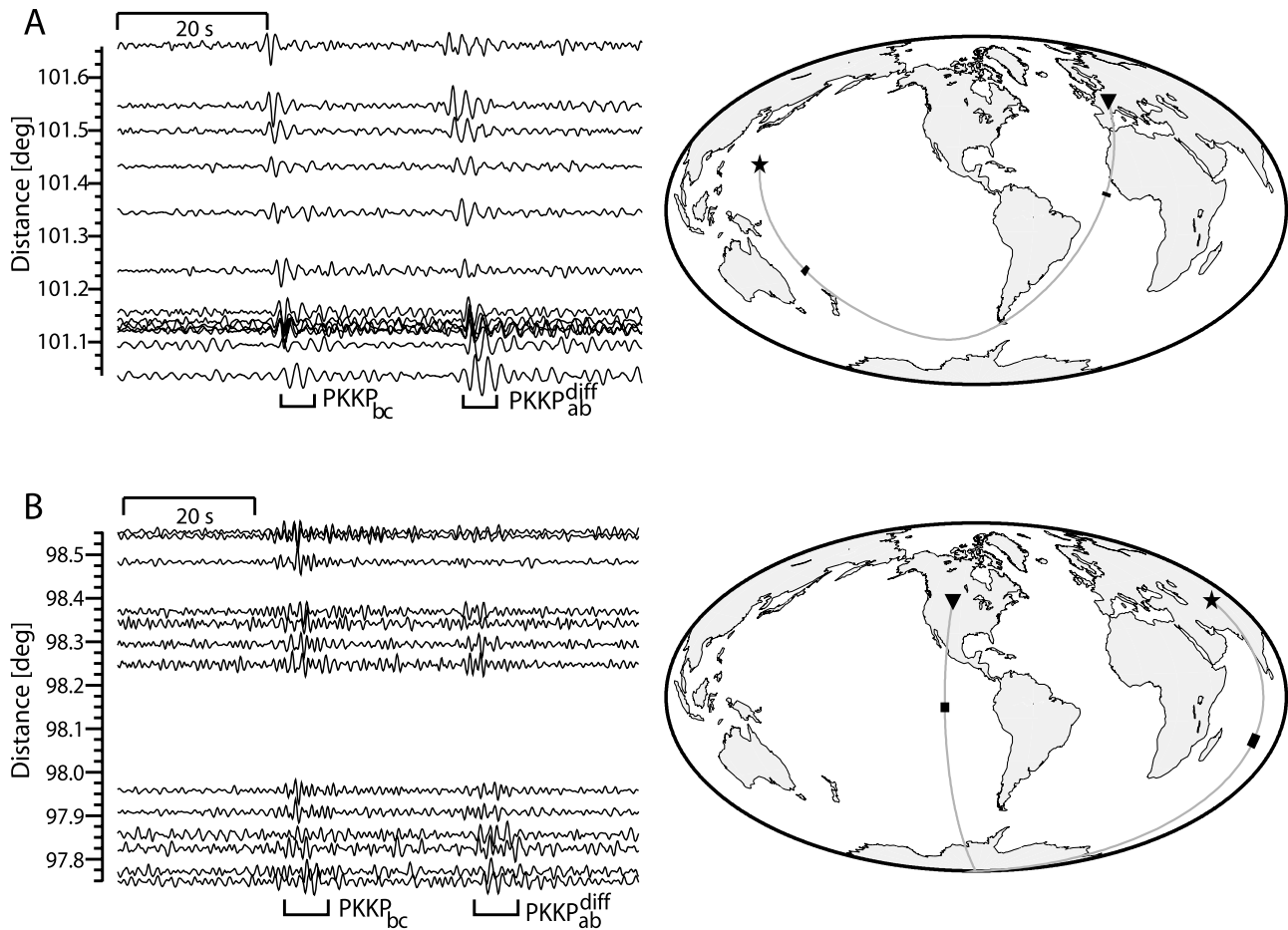


**Figure 8.** (a)  $PKKP$  time window of a Gräfenberg array (GRF) recording of an earthquake on 4 May 1988, 2347 UT. The minor arc distance is  $\sim 101.3^\circ$ . The distance profile clearly shows  $PKKP_{bc}$  and  $PKKP_{ab}^{diff}$  arrivals. The panel on the right shows the source-receiver geometry for this event. (b) Recordings of  $PKKP_{bc}$  and  $PKKP_{ab}^{diff}$  from the Large-Aperture Seismic Array (LASA) in an earthquake on 4 September 1972, 1342 UT. Only the records from the three innermost rings of LASA are shown. Because of the large number of stations we sum the LASA recordings in  $0.05^\circ$  distance steps. The distance range to LASA is approximately  $98.1^\circ$ . The panel to the right presents source-receiver combination for this event.

$SP_{diff}KS$ , to reduce the inherent source-receiver ambiguity of these probes is desirable, and will be pursued in future work.

[26] Preliminary studies using data from different arrays (e.g., Large Aperture Seismic Array (LASA) [Frosch and Green, 1966] and Gräfenberg Array (GRF) [Buttkus, 1986]) show that the strong  $PKKP_{ab}^{diff}$  arrivals for distances about  $7.5^\circ$  past the ray theoretical cutoff distance as documented in this manuscript for YKA are present elsewhere (Figure 8). This shows that recordings of this phase from arrays with varying apertures can be widely used to improve ULVZ detection and characterization, a necessary and important step for a better understanding of the role ULVZs play in large and small-scale mantle dynamics.

[27] **Acknowledgments.** We thank The Geological Survey of Canada for providing the Yellowknife data. Most figures were produced using GMT [Wessel and Smith, 1998]. We thank Keith Koper, Jeroen Ritsema, and an anonymous reviewer for thoughtful reviews, all which improved the manuscript. The work was partially funded by NSF grant EAR-0135119 and NSF grant EAR-0456356.

## References

- Bank, C.-G., M. G. Bostock, R. M. Ellis, and J. F. Cassidy (2000), A reconnaissance teleseismic study of the upper mantle and transition zone beneath the Archean Slave Craton in NW Canada, *Tectonophysics*, *319*, 151–166.
- Bataille, K., and F. Lund (1996), Strong scattering of short-period seismic waves by the core-mantle boundary and the  $P$ -diffracted wave, *Geophys. Res. Lett.*, *23*, 2413–2416.
- Bondar, I., R. G. North, and G. Bell (1999), Teleseismic slowness-azimuth station corrections for the International Monitoring System seismic network, *Bull. Seismol. Soc. Am.*, *89*, 989–1003.
- Buffett, B. A., E. J. Garnero, and R. Jeanloz (2000), Sediments at the top of Earth's core, *Science*, *290*, 1338–1342.
- Buttkus, B. (1986), Ten years of the Gräfenberg array, *Geol. Jahrb. Reihe E*, *35*, 135 pp.
- Capon, J. (1973), Signal processing and frequency-wavenumber spectrum analysis for a large aperture seismic array, *Methods Comput. Phys.*, *13*, 1–59.
- Castle, J. C., and R. D. van der Hilst (2000), The core-mantle boundary under the Gulf of Alaska: No ULVZ for shear waves, *Earth Planet. Sci. Lett.*, *176*, 311–321.
- Doornbos, D. J. (1980), The effect of a rough core-mantle boundary on  $PKKP$ , *Phys. Earth Planet. Inter.*, *21*, 351–358.
- Dziewonski, A. M., and D. L. Anderson (1981), Preliminary reference Earth model (PREM), *Phys. Earth Planet. Inter.*, *25*, 297–356.

- Earle, P. S., and P. M. Shearer (1997), Observations of PKKP precursors used to estimate small-scale topography of the core-mantle boundary, *Science*, *277*, 667–670.
- Frosch, R. A., and P. E. Green (1966), The concept of the large aperture seismic array, *Proc. R. Soc. London, Ser. A*, *290*, 368–384.
- Garnero, E. J. (2000), Heterogeneities of the lowermost mantle, *Annu. Rev. Earth Planet. Sci.*, *28*, 509–537.
- Garnero, E. J., and D. V. Helmberger (1996), Seismic detection of a thin lateral varying boundary layer at the base of the mantle beneath the central-Pacific, *Geophys. Res. Lett.*, *23*, 977–980.
- Garnero, E. J., S. Grand, and D. V. Helmberger (1993), Low *P*-wave velocity at the base of the mantle, *Geophys. Res. Lett.*, *20*, 1843–1846.
- Garnero, E. J., J. Revenaugh, Q. Williams, T. Lay, and L. H. Kellogg (1998), Ultralow velocity zones at the core-mantle boundary, in *The Core-Mantle Boundary, Geodyn. Ser.*, vol. 28, edited by M. Gurnis et al., pp. 319–334, AGU, Washington, D. C.
- Garnero, E. J., M. S. Thorne, A. McNamara, and S. Rost (2006), Fine-scale ultra-low velocity zone layering at the core-mantle boundary and superplumes, in *Superplumes: Beyond Plate Tectonics*, edited by D. A. Yuen et al., Springer, New York, in press.
- Hedlin, M. A. H., and P. M. Shearer (2000), An analysis of large-scale variations in small-scale mantle heterogeneity using Global Seismographic Network recordings of precursors to PKP, *J. Geophys. Res.*, *105*, 13,655–13,673.
- Helmberger, D. V., L. Wen, and X. Ding (1998), Seismic evidence that the source of the Iceland hotspot lies at the core-mantle boundary, *Nature*, *396*, 251–255.
- Helmberger, D. V., S. Ni, L. Wen, and J. Ritsema (2000), Seismic evidence for ULVZ beneath Africa and eastern Atlantic, *J. Geophys. Res.*, *105*, 23,865–23,878.
- Kárason, H., and R. D. van der Hilst (2001), Tomographic imaging of the lowermost mantle with differential times of refracted and diffracted core phases (PKP,  $P_{diff}$ ), *J. Geophys. Res.*, *106*, 6569–6587.
- Kendall, J. M. (2000), Seismic anisotropy in boundary layers of the mantle, in *Earths' Deep Interior: Mineral Physics and Tomography From the Atomic to the Global Scale, Geophys. Monogr. Ser.*, vol. 177, edited by S. I. Karato et al., pp. 133–159, AGU, Washington, D. C.
- Kendall, J. M., and P. G. Silver (1996), Constraints from seismic anisotropy on the nature of the lowermost mantle, *Nature*, *381*, 409–412.
- Krüger, F., and M. Weber (1992), The effect of low velocity sediments on the mislocation vectors of the GRF array, *Geophys. J. Int.*, *108*, 387–393.
- Lay, T., and D. V. Helmberger (1983), A lower mantle *S*-wave triplication and the shear velocity structure of  $D''$ , *Geophys. J. R. Astron. Soc.*, *75*, 799–838.
- Lay, T., Q. Williams, E. J. Garnero, L. Kellogg, and M. E. Wyssession (1998), Seismic wave anisotropy in the  $D''$  region and its implications, in *The Core-Mantle Boundary, Geodyn. Ser.*, vol. 28, edited by M. Gurnis et al., pp. 299–318, AGU, Washington, D. C.
- Lay, T., E. J. Garnero, and Q. Williams (2004), Partial melting in a thermochemical boundary layer at the base of the mantle, *Phys. Earth Planet. Inter.*, *146*, 441–467.
- Lay, T., D. Heinz, M. Ishii, S.-H. Shim, J. Tsuchiya, R. Wentzcovitch, and D. Yuen (2005), Multidisciplinary impact of the deep mantle phase transition in perovskite structure, *Eos Trans. AGU*, *86*(1), 1, 5.
- McNamara, A. K., and S. Zhong (2004), Thermochemical structures within a spherical mantle: Superplumes or piles?, *J. Geophys. Res.*, *109*, B07402, doi:10.1029/2003JB002847.
- McNamara, A. K., and S. Zhong (2005), Thermochemical piles beneath Africa and the Pacific, *Nature*, *437*, 1136–1139.
- Mori, J., and D. V. Helmberger (1995), Localized boundary layer below the mid-Pacific velocity anomaly identified from a *PcP* precursors, *J. Geophys. Res.*, *100*, 20,359–20,365.
- Mula, A. H., and G. Müller (1980), Ray parameters of diffracted long-period *P* and *S* waves and the velocity and *Q* structure at the base of the mantle, *J. Geophys. Res.*, *86*, 4999–5011.
- Murakami, M., K. Hirose, K. Kawamura, N. Sata, and Y. Ohishi (2004), Post-perovskite phase transition in  $MgSiO_3$ , *Science*, *304*, 855–858.
- Ni, S., and D. V. Helmberger (2003), Seismological constraints on the South African superplume: Could be the oldest distinct structure on Earth, *Earth Planet. Sci. Lett.*, *206*, 119–131.
- Okal, E. A., and R. J. Geller (1979), Shear wave velocity at the base of the mantle from profiles of diffracted SH waves, *Bull. Seismol. Soc. Am.*, *69*, 1039–1053.
- Persh, S. E., J. E. Vidale, and P. S. Earle (2001), Absence of short-period ULVZ precursors to *PcP* and *ScP* from two regions of the CMB, *Geophys. Res. Lett.*, *28*, 387–390.
- Revenaugh, J., and R. Meyer (1997), Seismic evidence of partial melt within a possibly ubiquitous low-velocity layer at the base of the mantle, *Science*, *277*, 670–673.
- Rost, S., and J. Revenaugh (2001), Seismic detection of rigid zones at the top of the core, *Science*, *294*, 1911–1914.
- Rost, S., and J. Revenaugh (2003a), Small-scale ultra-low velocity zone structure imaged by *ScP*, *J. Geophys. Res.*, *108*(B1), 2056, doi:10.1029/2001JB001627.
- Rost, S., and J. Revenaugh (2003b), Detection of a  $D''$  discontinuity in the south Atlantic using PKKP, *Geophys. Res. Lett.*, *30*(16), 1840, doi:10.1029/2003GL017585.
- Rost, S., and M. Weber (2001), A reflector at 210 km depth beneath the NW Pacific, *Geophys. J. Int.*, *147*, 12–28.
- Rost, S., E. J. Garnero, Q. Williams, and M. Manga (2005), Seismic constraints on a possible plume root at the core-mantle boundary, *Nature*, *435*, 666–669.
- Schimmel, M., and H. Paulssen (1997), Noise reduction and detection of weak coherent signals through phase weighted stacks, *Geophys. J. Int.*, *130*, 497–505.
- Tackley, P. (2002), Strong heterogeneity caused by deep mantle layering, *Geochim. Geophys. Geosyst.*, *3*(4), 1024, doi:10.1029/2001GC000167.
- Thorne, M. S., and E. J. Garnero (2004), Inferences on ultralow-velocity zone structure from a global analysis of *SPdKS* waves, *J. Geophys. Res.*, *109*, B08301, doi:10.1029/2004JB003010.
- Thorne, M. S., E. J. Garnero, and S. Grand (2004), Geographic correlation between hot spots and deep mantle lateral shear-wave velocity gradients, *Phys. Earth Planet. Inter.*, *146*, 47–63.
- Vidale, J. E., and M. A. H. Hedlin (1998), Evidence for partial melt at the core-mantle boundary north of Tonga from the strong scattering of seismic waves, *Nature*, *391*, 682–685.
- Wang, Y., and L. Wen (2004), Mapping the geometry and geographic distribution of a very low velocity province at the base of the Earth's mantle, *J. Geophys. Res.*, *109*, B10305, doi:10.1029/2003JB002674.
- Wen, L. (2001), Seismic evidence for a rapidly-varying compositional anomaly at the base of the Earth's mantle beneath the Indian Ocean, *Earth Planet. Sci. Lett.*, *194*, 83–95.
- Wen, L., and D. V. Helmberger (1998), A two-dimensional *P-SV* hybrid method and its application to modeling localized structures near the core-mantle boundary, *J. Geophys. Res.*, *103*, 17,901–17,918.
- Wen, L., P. Silver, D. James, and R. Kuehnel (2001), Seismic evidence for a thermochemical boundary layer at the base of the Earth's mantle, *Earth Planet. Sci. Lett.*, *189*, 141–153.
- Wessel, P., and W. H. F. Smith (1998), New, improved version of Generic Mapping Tools released, *EOS Trans. AGU.*, *79*(47), 579.
- Wyssession, M. E. (1996), Large-scale structure at the core-mantle boundary from core-diffracted waves, *Nature*, *382*, 244–248.
- Wyssession, M. E., and E. A. Okal (1989), Regional analysis of  $D''$  velocities from the ray parameters of diffracted *P* profiles, *Geophys. Res. Lett.*, *16*, 1417–1420.
- Wyssession, M. E., T. Lay, J. Revenaugh, Q. Williams, E. J. Garnero, R. Jeanloz, and L. H. Kellogg (1998), The  $D''$  discontinuity and its implications, in *The Core-Mantle Boundary, Geodyn. Ser.*, vol. 28, edited by M. Gurnis et al., pp. 273–298, AGU, Washington, D. C.
- Wyssession, M. E., A. Langenhorst, M. J. Fouch, K. M. Fischer, G. I. Al-Eqabi, P. J. Shore, and T. J. Clarke (1999), Lateral variations in compressional/shear velocities at the base of the mantle, *Science*, *284*, 120–125.
- Young, C. J., and T. Lay (1990), Multiple phase analysis of the shear velocity structure in the  $D''$  region beneath Alaska, *J. Geophys. Res.*, *95*, 17,385–17,402.

E. J. Garnero and S. Rost, Department of Geological Sciences, Arizona State University, Tempe, AZ 85287-1404, USA. (srost@asu.edu)